SANDIA REPORT

SAND2011-0582
Unlimited Release
Printed February 2011

Velocimetry signal synthesis with fringen

Daniel H. Dolan

Sandia National Laboratories

Issued by Sandia National Laboratories, operated for the United States Department of Energy by Sandia Corporation.

Printed in the United States of America. This report has been reproduced directly from the best available copy.

Available to DOE and DOE contractors from
     U.S. Department of Energy
     Office of Scientific and Technical Information
     P.O. Box 62
     Oak Ridge, TN 37831

Telephone:	(865) 576-8401
Facsimile:	(865) 576-5728
E-Mail:	reports@adonis.osti.gov
Online ordering:	http://www.osti.gov/bridge

Available to the public from
     U.S. Department of Commerce
     National Technical Information Service
     5285 Port Royal Rd
     Springfield, VA 22161

Telephone:	(800) 553-6847
Facsimile:	(703) 605-6900
E-Mail:	orders@ntis.fedworld.gov
Online ordering:	http://www.ntis.gov/help/ordermethods.asp?loc=7-4-0#online

Velocimetry signal synthesis with fringen

Daniel H. Dolan

Sandia National Laboratories

P.O. Box 5800

Albuquerque, NM 87185-1195

Abstract

An important part of velocimetry analysis the recovery of a known velocity history from simulated data signals. The fringen program synthesizes VISAR and PDV signals, given a specified velocity history, using exact formulations for the optical signal. Time-dependent light conditions, non-ideal measurement conditions, and various diagnostic limitations (noise, etc.) may be incorporated into the simulated signals.

Acknowledgements

The fringen program evolved from a set of MATLAB utilities for other programs, such as PointVISAR. Testing these programs required velocimetry signals that correspond with a known velocity history. It became tedious to manually create these synthetic signals, so I began to formalize these code fragments into a common function. This process accelerated during the development of THRIVE (SAND2008-3871), where a set of formal benchmark problems were required.

The operation and features of fringen was motivated by conversions with Scott Jones, Brian Jensen, and David Holtkamp. Documentation for this project was instigated by Phillip Rae.

Contents

Figures

Tables

1   Introduction

Optical velocimetry generally involves inverse analysis: a reflector's velocity history is inferred from a set of acquired data signals. While great efforts are spent in making this process robust, inverse analysis is based on assumptions. A common assumption is that reflector's velocity is nearly constant over small time durations; common detector response at all frequencies is another standard assumption. The validity of these assumptions becomes suspect as velocimetry measurements move to shorter time scales.

Forward analysis, where velocimetry signals are synthesized from a known velocity history, can be performed in a theoretically exact fashion. Various non-ideal behavior may be incorporated into forward analysis, including extreme accelerations, variable light conditions, frequency-dependent detector response, unbalanced velocimetry signals, signal noise, and digitizer limitations. While forward analysis is not necessarily unique (different velocity histories may yield similar synthetic data signals), it provides physical intuition for how various factors and settings affect velocimetry signals. Furthermore, forward analysis allows rigorous benchmarking for data reduction codes.

This report describes the fringen program, which performs forward VISAR (Velocity Interferometer System for Any Reflector [1]) and PDV (Photonic Doppler Velocimetry, also known as heterodyne velocimetry [2]) analysis. Nearly all effects that might occur in VISAR/PDV measurement of a single velocity can be modeled by fringen. The program operates in MATLAB, either within a graphical interface or as a user-callable function. The current stable version of fringen is 0.3, which was released in October 2010.

The following sections describe the operation and use of fringen. Section 2 gives a brief overview of VISAR and PDV synthesis. Section 3 illustrates the graphical and console interface of fringen. Section 4 presents several example uses of the program. Section 5 summarizes program capabilities and discusses potential future work.

2   Signal generation

Detailed descriptions of VISAR [3] and PDV [4, 5] operation are given elsewhere, so only a brief summary is presented here. Both measurements rely on the interference of two optical signals [6], yielding an interference intensity $I(t)$:

$$I(t) = I_1(t) + I_2(t) + 2\sqrt{I_1(t)I_2(t)}\cos\Phi(t) \tag{1}$$

where the interpretation of I_1, I_2, and Φ depends on the interferometer configuration. The output signal $s(t)$ is a product of optical effects in the interferometer and electrical effects in the measured signal(s).

2.1   Optical effects

The optical outputs in VISAR/PDV measurements depend on several factors. Presumably most important is the reflector's motion, though the amount and type of light present in the measurement plays a role. Mixing of light from the two paths of the interferometer is also important. Relative phase shifts, introduced in multi-signal measurements, are another contribution to the optical output(s). Each of these effects is described below.

Given a velocity history $v(t)$, reflector position $x(t)$ may be inferred by numerical integration (assuming $x = 0$ at time $t = 0$). A VISAR observing this motion will produce a phase difference:

$$\Phi(t) = \frac{4\pi}{\lambda_0}\big[x(t) - x(t-\tau) + \delta\tau v(t-\tau)\big] + \Phi_R \tag{2}$$

where τ is the interferometer delay and δ is the interferometer dispersion.[1] A PDV observing the same motion will see a different phase difference:

$$\Phi(t) = \frac{4\pi}{\lambda_0}x(t) + \Phi_R + 2\pi f_s t \tag{3}$$

where f_s is the shift frequency [5]. Both interferometer configurations have a reference phase difference Φ_R, which determines the signal phase at time $t = 0$.

Coherent light from the reflector during a velocimetry measurement has an optical intensity $I_C(t)$, which may vary either because of the optical source (*e.g*, pulsed laser) or variable target return (reflectivity changes, probe efficiency, etc.). The reflector (or its surroundings) may also emit incoherent light with intensity $I_E(t)$ during the measurement. For a VISAR measurement, Equation 1 is thus modified as:

$$\begin{aligned} I_1(t) + I_2(t) &\to I_T(t) + I_E(t) \\ \sqrt{I_1(t)I_2(t)} &\to I_T(t) \end{aligned} \qquad \text{(VISAR)}$$

where it is assumed that variations in I_T and I_E are slow compared to the interferometer delay time. PDV measurements contain a third optical input, reference intensity $I_R(t)$ (which is almost

---

[1]This expression is exact, unlike the more common VISAR approximation [3].

always constant), leading to a different modification of Equation 1.

$$I_1(t) + I_2(t) \rightarrow I_T(t) + I_E(t) + I_R$$
$$\sqrt{I_1(t)I_2(t)} \rightarrow \sqrt{I_T(t)I_R} \qquad \text{(PDV)}$$

Baseline VISAR and PDV optical signals vary with target intensity, but signal amplitude is a different matter. VISAR amplitudes vary with target intensity, while PDV amplitudes vary with the square root of target intensity.

Mixing from the two optical paths in VISAR and PDV measurements may be further altered by balancing. For example, the beamsplitter used in a VISAR may perfectly split light between the reference and delay leg, causing an imbalance of optical intensities at the output. Introducing a set of balancing parameters into Equation 1 accounts for such differences.

$$I_1(t) + I_2(t) \rightarrow (a+b)\left(I_T(t) + I_E(t)\right)$$
$$\sqrt{I_1(t)I_2(t)} \rightarrow I_T(t)\sqrt{ab} \qquad \text{(VISAR)}$$
$$I_1(t) + I_2(t) \rightarrow a\left(I_T(t) + I_E(t)\right) + bI_R$$
$$\sqrt{I_1(t)I_2(t)} \rightarrow \sqrt{abI_T(t)I_R} \qquad \text{(PDV)}$$

Coefficient a refers to the longer (delay) path of a VISAR or the target path of a PDV, while coefficient b refers to shorter path in a VISAR or the reference path in a PDV.

A final variation in VISAR and PDV is the use of multi-phase measurements. For example, VISAR is traditionally performed with two quadrature signals. Each signal can be represented with its own version of Equation 1. The reference phase of the k-th signal is shifted by an amount β_k:

$$\Phi_R \rightarrow \Phi_R - \beta_k$$

to account for phase shifts introduced by the VISAR or PDV. A two-signal VISAR would have have phase shifts $\beta_1 = 0$ and $\beta_2 = 90°$ (nominal values), while a four-signal VISAR could have phase shifts $\beta_1 = 0$, $\beta_2 = 180°$, $\beta_3 = 90$, and $\beta_4 = 270°$ (depending on convention).

Each phase shift β_k is associated with coupling parameters a_k and b_k. Interference within a particular VISAR/PDV signal is dictated by the ratio a_k/b_k, while the relative signal magnitudes are defined by the ratio a_k/a_m $(k \neq m)$. This effect can be used to model detectors with different responsivities. For example, a balanced two-signal VISAR $(a_k = b_k)$ with one "hot" detector can be represented by $a_1 = b_1 = 1$ and $a_2 = b_2 = 2$, making variations in the second signal twice as large as the first signal.

2.2 Electrical effects

The optical output $I(t)$ of an interferometer is converted to an electrical signal $s(t)$ for digital acquisition and subsequent processing. Four modifications to this process are considered here. First, the detector may be DC or AC coupled to the digitizer, modifying the signal baseline. The signal may be then passed through a linear transfer function, defined by an impulse response curve, to mimic the frequency response of a real detector. Next, the signal may be corrupted by

9

noise. Finally, the analog signal is converted to a discrete, digital representation. Basic models for each process are described below. This discussion is not meant to be all-encompassing, and some important details have been omitted.

Detectors used in velocimetry may be DC or AC coupled. DC coupling is generally, though not universally, used in VISAR measurements to preserve a reference state at zero velocity. AC coupling is quite common in the high-speed detectors required by PDV, and may be quite beneficial in variable light-level measurements (see Example 3) to remove large reference intensities. A crude model for AC coupling assumes that the average signal present at times $t < 0$ has always existed. This average signal charges a conceptual blocking capacitor, and it thus removed from the output. Quantitatively, this may be expressed as follows.

$$s(t) = I(t) - \frac{1}{|t_s|} \int_{t_s}^{0} I(t) \ dt \tag{4}$$

Velocity histories should be specified to be zero from a starting time $t_s < 0$, placing all motion of interest at $t \geq 0$. If PDV signals vary prior to $t = 0$, as in the case of frequency-conversion, several cycles should be placed in the starting time interval to correctly simulate an AC measurement.

Finite electrical bandwidth (detector or digitizer) affects the transduction of optical intensity to electrical signal. This process can be modeled through a linear transfer function $H(f)$, which maps the optical input to an electrical output at a particular frequency. For example, a low-pass RC filter has a transfer function:

$$H(f) = \frac{1}{1 + 2\pi i f \tau} \tag{5}$$

where τ is the characteristic response time. The output signal $s_{\text{out}}(t)$ is a convolution of $H(f)$ with the input signal, a process that be carried out in the frequency or time domain. Since $H(f)$ may be a complex-value function, it is procedurally simpler to deal with the impulse response function $h(t)$, which is equivalent to the Fourier transform of $H(f)$ [7].

$$h(t) \propto \int_{0}^{\infty} \text{Re}\left[H(f)\right] \cos(2\pi f t) \ df \qquad t > 0 \tag{6}$$

The impulse response of the low-pass filter described above is proportional to $e^{-t/\tau}$ for $t \geq 0$ (and zero otherwise).

Signal noise is an important but potentially confusing topic in forward velocimetry analysis. A very specific concept of noise fraction—the root-mean-square variation of the signal relative to the overall signal amplitude—is used here. Consider a harmonic signal containing random noise.

$$y(t) = A \cos(2\pi f t + \delta) + \sigma A R(t) \tag{7}$$

Over many cycles, this signal has an average amplitude A, but any any given time the signal is perturbed by a random function $R(t)$. The mean value of $R(t)$ is zero, but its variance is unity, giving the signal a noise fraction of σ. This effect is implemented in fringen by estimating A from the total optical signal variation (half the difference between minimum and maximum $I(t)$) and drawing $R(t)$ from a normally-distributed pseudorandom generator (MATLAB's `randn` function). The generator can be seeded with a specific key to obtain reproducible noise signals.

10

Digitizing VISAR and PDV signals invariably causes precision loss. Consider a measurement where the electrical signal is perfectly bound between minimum s_A and maximum s_B with N effective bits. Scaling the signal between zero and unity, multiplying by the maximum bit level and rounding to the nearest integer simulates the sampling process.

$$d(t) = \text{round}\left[(2^N - 1)\frac{s(t) - s_A}{s_B - s_A}\right] \tag{8}$$

$$s_d(t) = s_A + \left[\frac{s_B - s_A}{2^N - 1}\right]d(t) \tag{9}$$

This calculation does not explicitly account for signals that do fully span the dynamic range of the digitizer, but such effects could be incorporated by setting N below the digitizer bit depth. Note that N need not be an integer!

3 Using fringen

The fringen program operates in MATLAB (release 2008a or later) on any computer platform. The program can also be compiled into an executable version. As of January 2011, frigen is licensed for government use. To obtain a copy of frigen, contact the author at `dhdolan@sandia.gov`.

The program operates in four general stages.

1. The user defines a velocity history through a data file.

2. The interferometer type (VISAR or PDV) and parameters (wavelength, etc.) are specified.

3. Defects, such as noise, are applied to the ideal signals.

4. The calculated signals are saved to a data file.

Each stage can be accessed interactively through a graphical interface, shown in Figure 1, by calling fringen without input arguments.

```
>> fringen; % launch graphical interface
```

Calling fringen with input arguments bypasses the graphical interface.

```
>> param=struct('wavelength',532e-9,'delay',1e-9)

param =

    wavelength: 5.3200e-07
         delay: 1.0000e-09

>> [signal,time]=fringen('VISAR','ramp1.txt',param); % bypass graphical interface
```

Up to three input arguments—the interferometer type, the velocity history, and a parameter structure—can be passed to the program. For more details, type "`help fringen`" at the MATLAB command prompt.

Velocity history input for fringen is specified by an ASCII data files containing 2–5 columns. The first two columns, time and velocity, are mandatory. No assumptions about units are made for either column—fringen expects the user to be consistent. Three additional columns (coherent, incoherent, and reference intensity) may also be specified to define dynamic light conditions; each column is optional but must be specified in order. For example, the coherent intensity history must be defined (even if constant) to specify an incoherent intensity history.

Table 1 summarizes the analysis parameters recognized by fringen. In the graphical interface, parameters are specified by dialog boxes located under the "Interferometer" and "Signal" menus; outside of the graphical interface, parameters are sent through a user-defined structure. Many
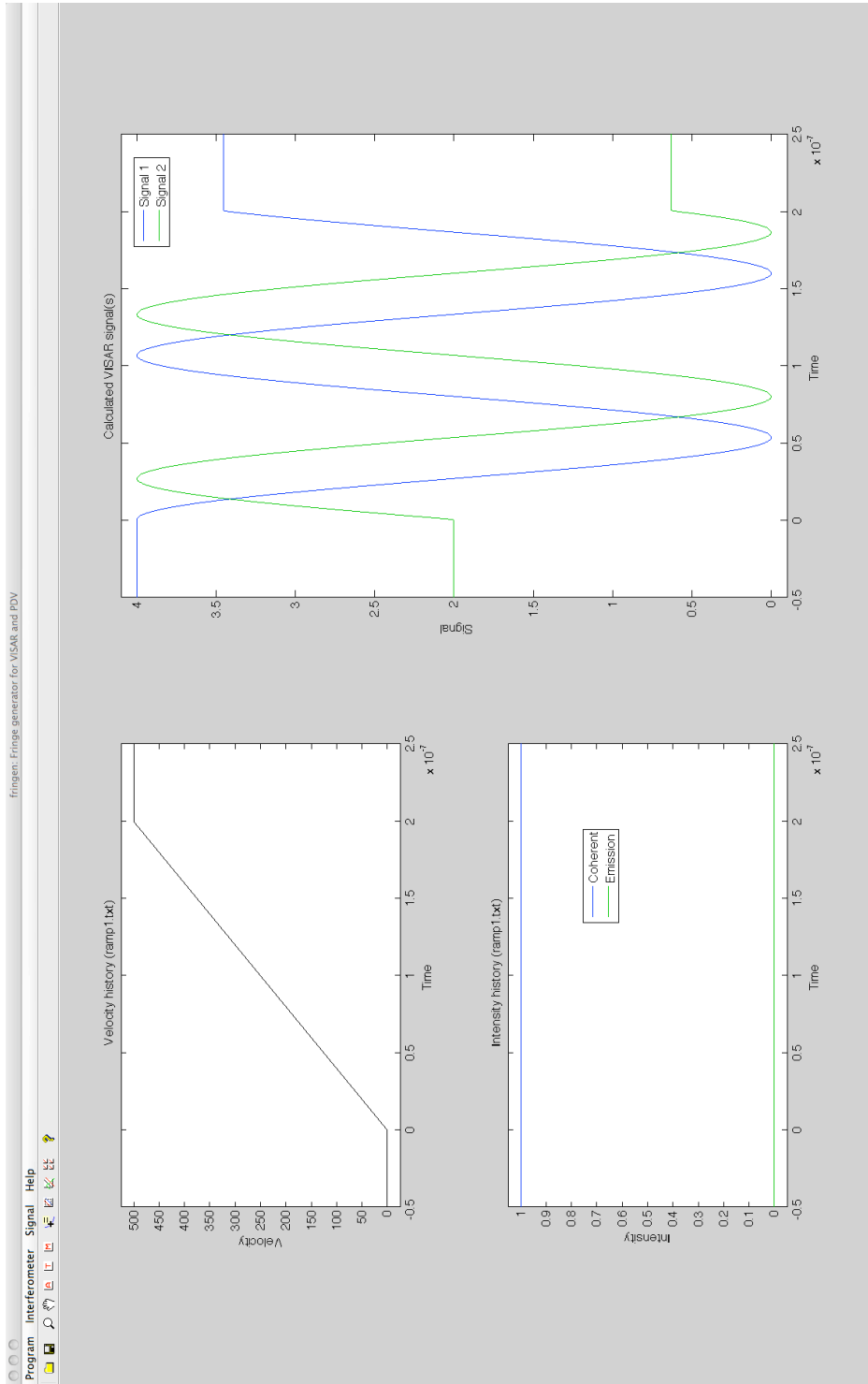
Figure 1. Graphical interface

Table 1. Summary of fringen parameters

Parameter	Default value	Description/comments
wavelength	variable	Laser wavelength
fshift[†]	0	Frequency shift
delay[*]	1E-9	Interferometer delay
dispersion[*]	0	Interferometer dispersion
ref_phase	0	Interference phase at $t = 0$
phase_shift	variable	Signal phase shift (degrees)
ref_scale	1	Reference-path scaling factor
delay_scale[*]	1	Delay-path scaling factor (VISAR)
target_scale[†]	1	Target-path scaling factor (PDV)
coupling	DC	Detector coupling
impulse_response	—	Data file containing an impulse response function
noise_fraction	0	Noise fraction
bit_range	8	Digitizer bit range
noise_seed	—	Random number generator seed

[*] VISAR only
[†] PDV only

of the parameters apply to both VISAR and PDV measurements, but several are configuration specific. Most fields have a default value, some of which are measurement dependent. For instance, the wavelength parameter defaults to 532e-9 for VISAR and 1550e-9 for PDV.

The number signals created by fringen is dictated by the number of entries for the phase_shift parameter. The default value of this field is [0 180 90 270] for VISAR and [0] for PDV (units of degrees). Greater or fewer signals can be specified at the user's discretion. Scaling factors (reference, target, and/or delay) are replicated as necessary to calculate all the signals defined by phase_shift.

Fields that have no default parameter, such as noise_seed, are associated with features that are normally dormant. Specifying a noise seed parameter resets the random number generator to a defined state for reproducible noise signals; otherwise, fringen uses the current generator state. The impulse_function field is used to specify the name of a text file (two columns, starting at time zero) containing an impulse response, which fringen uses to simulate detector transfer functions; no transfer calculations are performed when this field is omitted.
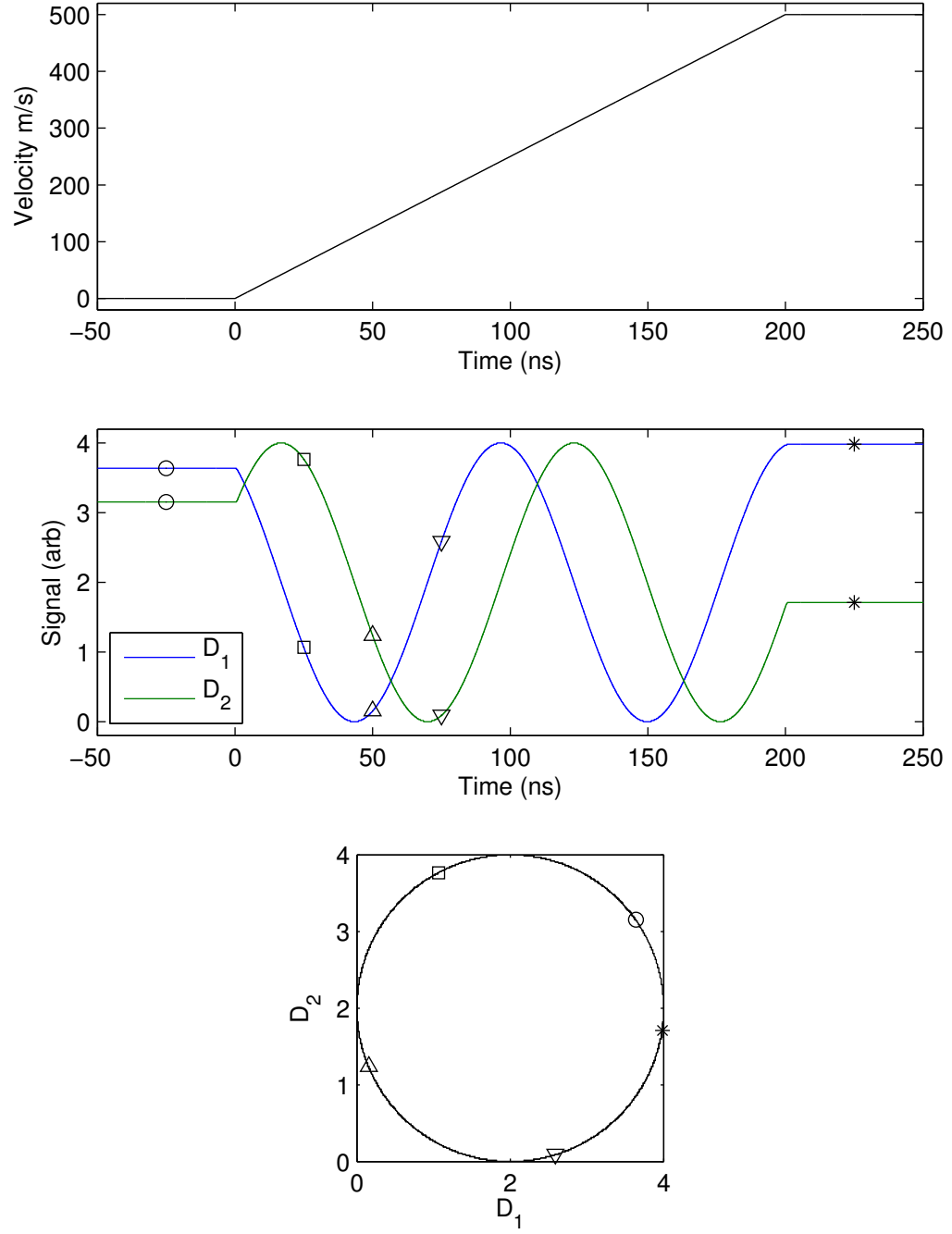
4   Examples

Three example uses of fringen are provided to illustrate how various system settings affect velocimetry signals. Each example is based on a ramp wave, illustrated in the top left portion of Figure 1), where a hypothetical reflector undergoes constant acceleration from zero to 500 m/s over 200 ns. The first two examples assume constant light conditions, defined in the data file `ramp1.txt`. The third example includes variable light conditions, defined in the data file `ramp2.txt`. Results presented here are stored in files `example1.out`, `example2.out`, `exampleA.out`, and `exampleB.out`. For visual clarity in this report, noise is omitted from the calculations.

Figure 2 shows a simulated pair of VISAR signals for the ramp wave described above. The VISAR system (operating at 532 nm) has a 1 ns delay time (266 m/s fringe constant) with zero dispersion and a 35° reference phase. The upper plot shows a quadrature signal pair, shifted by exactly 90°, as a function of time. The lower plot shows the second signal against the first, illustrating that the measurement traces an ellipse. The circle, square, triangle, and asterisk symbols in the upper plot are matched to the locations on the ellipse, indicating that the reflector's acceleration corresponds to counterclockwise motion on the VISAR ellipse. In this particular example, the measurement sweeps the ellipse just under two times, which one expects for a 500 m/s velocity change with a 266 m/s fringe constant (1.88 fringes).

Figure 3 shows a simulated PDV signal for a ramp wave using AC coupling. An obvious result of this calculation is that the signal fringes get closer together as ramp velocity increases, *i.e.* the beat frequency is proportional to velocity (as expected [2]). Closer inspection reveals that the signal baseline vertically "hops" away from the zero at the onset of motion. This effect is often seen in AC coupled measurements, and has to do with the fact that static interference (defined by the reference phase shift) in the PDV may be masked by the AC coupling. If the digitizer sensitivity limits are set too tightly, this effect can lead to unexpected clipping during a measurement.

Figure 4 shows two simulated PDV signals for a ramp wave with variable light conditions. The simulations include a modest frequency shift (10 MHz), which eliminates the baseline hop while retaining discernible fringes on a plot spanning 2500 ns; on this scale, individual fringes are difficult to visually resolve shortly after motion begins. At time $t = 500$ ns, the simulations allows coherent light levels from the target to linearly increase up to twice the original value, stopping at $t = 1000$ ns. Some time later ($t =$1250 ns), the simulations incorporate incoherent emission, which persists until $t = 1750$ ns.

The first simulation in Figure 4 assumes that equal levels of target and reference light interfere at the PDV detector. Equal light levels were also assumed in the previous two examples, and this configuration is commonly sought in VISAR measurements to achieve high optical contrast (leading to complete destructive interference as in Figure 2). Balanced target and reference light levels are not necessarily important in PDV measurements, and can in fact be detrimental. Optically balanced PDV signals undergo both a change in amplitude and baseline when target light levels change, and configuring a digitizer to accommodate these changes sacrifices dynamic range. Feeding substantially more reference than target light to the PDV detector circumvents the problem (if AC coupling is present to present to reject the reference baseline). The second simulation in Figure 4 shows a measurement with reference scaling set to 10 and target scaling set to 0.1. The overall fringe amplitude is preserved in the second simulation, but the baseline does not vary nearly as

Figure 2. Example 1: (upper) input ramp velocity history; (middle) simulated VISAR signals; (bottom) VISAR ellipse.
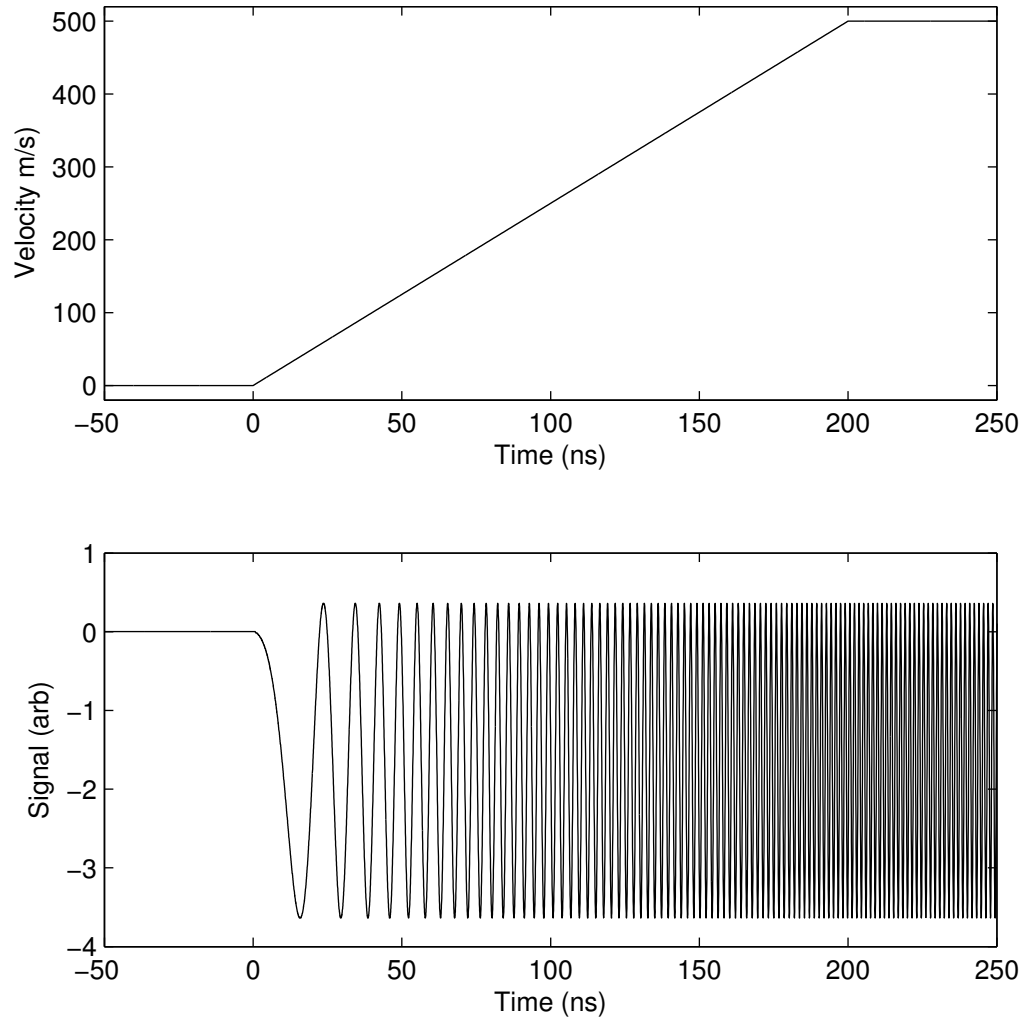
Figure 3. Example 2: (upper) input ramp velocity history; (lower) simulated PDV signal with AC coupling.

much as in the first simulation. There are practical limits to how much reference light can be used in a PDV measurement: too much will make the detector behave nonlinearly and eventually saturate. As a general rule of thumb, 10–100$\times$ more reference light than target light is a practical goal.
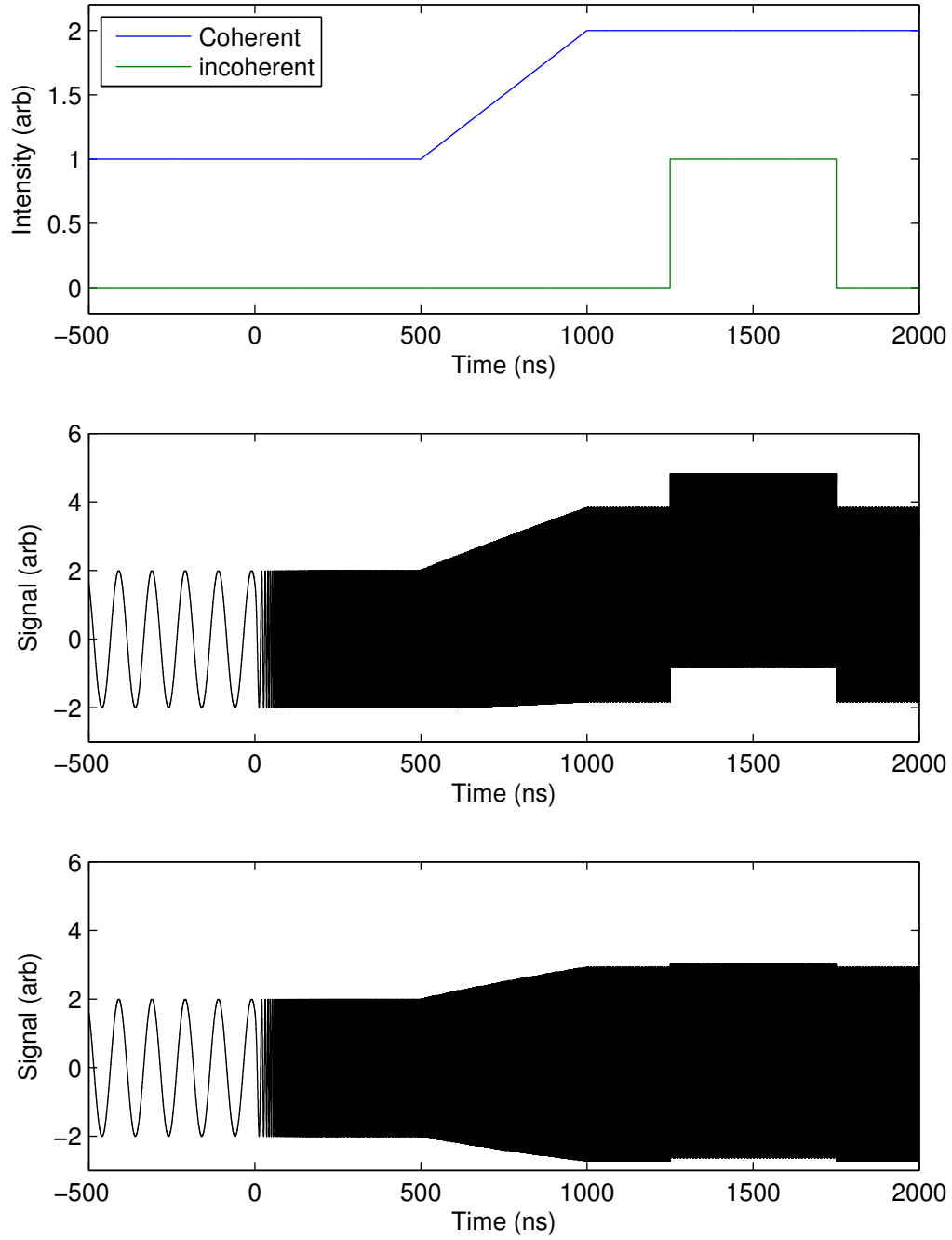
Figure 4. Example 3: (upper) variable light history; (middle) simulated PDV signal with balanced target/reference light; (lower) simulated PDV signal with imbalanced target/reference light.

19

5 Summary and future work

Simulated VISAR and PDV signals can be created with the fringen program for a wide range of measurement conditions. Exact expressions are used to convert a specified velocity history to optical signals, providing rigorous benchmark tests for data reduction programs. Various optical and electrical measurement defects may be included in the simulated signals.

Version 0.3 of fringen supports nearly all perturbations that might be encountered in a single-velocity measurement. Enhancements to existing functions or new program features will be considered if there is sufficient user interest. Multiple, simultaneous velocity simulations are unlikely to be supported due to the immense complexity of the general problem. Approximations for multiple velocity effects can be obtain by summing independent fringen simulations (preferably outside of the graphical interface).

$$s(t) = \sum_k s_k(t) \tag{10}$$

Such summations are reasonably valid in many PDV measurements, where interference between different Doppler shifts is negligible.

References

[1] L.M. Barker and R.E. Hollenbach. Laser interferometer for measuring high velocities of any reflecting surface. *Journal of Applied Physics* **43**, 4669–4675 (1972).

[2] O.T. Strand and D.R. Goosman and C. Martinez and T.L. Whitworth. Compact system for high-speed velocimetry using heterodyne techniques. *Review of Scientific Instruments* **77**, 83108 (2006).

[3] D.H. Dolan. Foundations of VISAR analysis. Technical Report SAND2006-1950, Sandia National Laboratories, (2006).

[4] D.H. Dolan and S.C. Jones. THRIVE: a data reduction program for three-phase PDV/PDI and VISAR measurements. Technical Report SAND2008-3871, Sandia National Laboratories, (2008).

[5] T. Ao and D.H. Dolan. SIRHEN: a data reduction program for photonic Doppler velocimetry measurements. Technical Report SAND2010-3628, Sandia National Laboratories, (2010).

[6] M. Born and E. Wolf. *Principles of Optics*. Cambridge University Press, Cambridge, 7th edition, (1999).

[7] G.B. Arfken and H.J. Weber. *Mathematical Methods for Physicists*. Academic Press, San Diego, fourth edition, (1995).

DISTRIBUTION:

1   E. Daykin
    P.O. Box 98521
    National Security Technologies
    Las Vegas, NV 89193
1   E. Machorro
    P.O. Box 98521
    National Security Technologies
    Las Vegas, NV 89193
1   B. Marshall
    5520 "B" Ekwill Street
    Special Technologies Laboratory
    Santa Barbara, CA 93111
1   G. Stevens
    5520 "B" Ekwill Street
    Special Technologies Laboratory
    Santa Barbara, CA 93111

1   M. Briggs
    P.O. Box 1663
    Los Alamos National Laboratory
    Los Alamos, NM 87545
1   M. Furlanetto
    P.O. Box 1663
    Los Alamos National Laboratory
    Los Alamos, NM 87545
1   R. Gustavsen
    P.O. Box 1663
    Los Alamos National Laboratory
    Los Alamos, NM 87545
1   D. Holtkamp
    P.O. Box 1663
    Los Alamos National Laboratory
    Los Alamos, NM 87545
1   B. Jensen
    P.O. Box 1663
    Los Alamos National Laboratory
    Los Alamos, NM 87545
1   P. Rae
    P.O. Box 1663
    Los Alamos National Laboratory
    Los Alamos, NM 87545

1   R. Chau
    7000 East Ave
    Lawrence Livermore National Laboratory
    Livermore, CA 94550

1 N.C. Holmes
7000 East Ave
Lawrence Livermore National Laboratory
Livermore, CA 94550
1 O.T. Strand
7000 East Ave
Lawrence Livermore National Laboratory
Livermore, CA 94550

1	MS 1133	M.U. Anderson, 5916
1	MS 1157	K.J. Fleming, 54341
1	MS 1454	B.A. Jilek, 2554
1	MS 0425	S.C. Jones, 545
1	MS 0826	W.M. Trott, 1512
1	MS 1133	J. Podsednik, 5916
1	MS 1454	M.D. Willis, 2552
1	MS 9042	T.J. Vogler, 8246
1	MS 1193	R.G. Hacking, 16561
1	MS 1193	S.L. Payne, 16561
2	MS 1106	T. Ao, 1646
1	MS 1186	M. Herrmann, 1640
1	MS 1195	C.S. Alexander, 1646
1	MS 1195	J.-P. Davis, 1646
5	MS 1195	Daniel Dolan, 1646
1	MS 1195	D.H. Dalton, 1646
1	MS 1195	M.D. Furnish, 1646
1	MS 1195	R.J. Hickman, 1647
1	MS 1195	M.D. Knudson, 1646
1	MS 1195	C.J. Meyer, 1646
1	MS 1195	S. Root, 1646
1	MS 1195	W.D. Reinhart, 1646
1	MS 1195	J.L. Wise, 1646
1	MS 1205	C.A. Hall, 5902
1	MS 0899	Technical Library, 9536 (electronic copy)